

CONF-7906109--1

LA-UR -79-1954

TITLE: METHOD OF OPTIMAL TRUNCATION: A NEW  
T-MATRIX APPROACH TO ELASTIC WAVE SCATTERING

AUTHOR(S): William M. Visscher

SUBMITTED TO: Pergamon Press  
Focus on the T-Matrix Approach  
Ohio State University, Conference

**MASTER**

University of California

By acceptance of this article, the publisher recognizes that the U.S. Government retains a nonexclusive, royalty-free license to publish or reproduce the published form of this contribution, or to allow others to do so, for U.S. Government purposes.

The Los Alamos Scientific Laboratory requests that the publisher identify this article as work performed under the auspices of the U.S. Department of Energy.



**LOS ALAMOS SCIENTIFIC LABORATORY**

Post Office Box 1663 Los Alamos, New Mexico 87545

An Affirmative Action/Equal Opportunity Employer

DISTRIBUTION OF THIS DOCUMENT IS UNLIMITED

# METHOD OF OPTIMAL TRUNCATION: A NEW T-MATRIX APPROACH TO ELASTIC WAVE SCATTERING

William M. Visscher\*  
Theoretical Division, Los Alamos Scientific Laboratory  
Los Alamos, New Mexico 87545

**NOTICE**  
This report was prepared as an account of work sponsored by the United States Government. Neither the United States nor the United States Department of Energy, nor any of their employees, nor any of their contractors, subcontractors, or their employees, makes any warranty, express or implied, or assumes any legal liability or responsibility for the accuracy, completeness or usefulness of any information, apparatus, product or process disclosed, or represents that its use would not infringe privately owned rights.

## ABSTRACT

A family of matrix theories of elastic wave scattering is derived, and one, which is in a certain sense optimal, is developed. Called the method of optimal truncation (MOOT), it results from a minimum principle and can be shown to yield a convergent sequence of approximations. Numerical results for scattering cross-sections for longitudinal incident waves with  $ka \leq 10$  from fixed rigid obstacles and voids with axial symmetry are obtained using MOOT, and are compared with results of other matrix theories. Shapes considered include spheres, oblate and prolate spheroids, pillboxes, and cones. Convergence is demonstrated. Extension of the method to elastic and fluid inclusions is discussed, as is its application to cracks, which may be accomplished by simulating the crack with an incompletely bonded identical inclusion. Implications of reciprocity and time-reversal invariance are discussed.

## I. INTRODUCTION

Proliferation of important scientific and technological applications in geology, materials science, and nondestructive testing, coupled with the current ubiquity of large computers, has spurred the development of methods for calculating the scattering of elastic waves from flaws. In this paper we will consider some of these methods, in particular the so-called T-matrix theories (1,2,3). We derive a family of these theories in Section II, and consider the problem of picking out an optimal one in Section III. These methods usually involve an expansion of the scattered displacement field in a finite (truncated) sum of partial-waves, and they result in sets of linear equations for the partial-wave amplitudes.

A particular choice, resulting from imposing the requirement that it minimize the mean-square deviance from the boundary conditions, is shown in Section IV to yield a sequence of approximations which converges as the truncation limit  $L$  increases. We call this matrix theory MOOT, the method of optimal truncation. Numerical results from MOOT and other methods are presented and compared in Section V, for some examples wherein the flaw is an axially symmetric void or a fixed rigid obstacle of spheroidal, cylindrical, or conical shape, and the incident longitudinal wave has  $ka \leq 10$ . In Section VI the extension of MOOT to elastic and fluid inclusions, and to cracks, is discussed.

\*Supported by U.S. Department of Energy

William M. Visscher

## II. FAMILY OF MATRIX METHODS

Because they are simpler than the equations of elasticity (4), we will illustrate the methods with the equations of the incompressible irrotational fluid (5). In that case, if  $\phi(\vec{r}, t)$  is the velocity potential

$$\vec{v} = -\vec{\nabla} \phi, \quad (1)$$

then the linearized equation of motion for a homogeneous system is

$$\left( \nabla^2 - \frac{1}{c^2} \frac{\partial^2}{\partial t^2} \right) \phi(\vec{r}, t) = 0. \quad (2)$$

If harmonic time dependence is assumed, this becomes the Helmholtz equation

$$(\nabla^2 + k^2) \phi = 0, \quad (3)$$

where the wavenumber  $k$  is given by

$$k^2 = \omega^2/c^2 = \omega^2 \rho/\kappa. \quad (4)$$

$\kappa$  is the compressibility modulus,  $\rho$  is the equilibrium density, and the pressure is

$$P = \frac{\partial \phi}{\partial t} = i\omega \rho \phi. \quad (5)$$

If the fluid has within it an inclusion with different density and compressibility modulus  $\rho'$  and  $\kappa'$ , with volume  $V$  bounded by a surface  $\Sigma$  (see Fig. 1), then Eq. (3) with appropriately modified  $k$  will again be satisfied inside  $\Sigma$ . Continuity of pressure across the boundary requires

$$\rho' \phi(\vec{r}_-) = \rho \phi(\vec{r}_+) \quad (6)$$

(where  $\vec{r}_\pm$  are positions just outside and inside  $\Sigma$ , respectively), and conservation of matter demands

$$\hat{n} \cdot \vec{\nabla} \phi(\vec{r}_-) = \hat{n} \cdot \vec{\nabla} \phi(\vec{r}_+), \quad (7)$$

where  $\hat{n}$  is the unit outward normal to  $\Sigma$ .

The scattering solution of Eq. (3) which we seek has the form

$$\phi(\vec{r}) = \phi_{\text{inc}}(\vec{r}) + \sum_{\mathbf{s}} a_{\mathbf{s}} \phi_{\mathbf{s}}^{(+)}(\vec{r}), \quad (8)$$

where  $\phi_{\text{inc}}$  is an incident plane wave,  $\phi_{\mathbf{s}}^{(+)}$  is an outgoing spherical wave specified by eigenvalues  $\mathbf{s} = (\ell, m)$ , and  $a_{\mathbf{s}}$  is the corresponding complex amplitude.  $\phi_{\text{inc}}$  and  $\phi_{\mathbf{s}}^{(+)}$  are solutions of Eq. (3). In detail,

$$\phi_{\text{inc}}(\vec{r}) = e^{i\vec{k}_o \cdot \vec{r}} = \sum_{\mathbf{s}} d_{\mathbf{s}} \check{\phi}_{\mathbf{s}}(\vec{r}) = 4\pi \sum_{\ell, m} i^{\ell} Y_{\ell m}^*(\theta_o, \phi_o) Y_{\ell m}(\theta, \phi) j_{\ell}(kr), \quad (9)$$

$$\phi_{\mathbf{s}}^{(+)} = \phi_{\ell m}^{(+)} = h_{\ell}^{(1)}(kr) Y_{\ell m}(\theta, \phi), \quad (10)$$

MOOT

where the spherical Hankel function  $h_\rho^{(1)} = j_\rho + iy_\rho$  in terms of the spherical Bessel and Neumann functions, and

$$\tilde{\phi}_s = \tilde{\phi}_{\rho m} = j_\rho(kr)Y_{\rho m}(\theta, \phi) \quad (11)$$

is the part of  $\phi_s^{(+)}$  which is regular at the origin.  $Y_{\rho m}$  is the usual spherical harmonic (6).

The partial-wave amplitudes  $a_s$  in Eq. (8) specify the outgoing wave from which the scattering cross-sections may be calculated. We will now derive, in a nearly trivial way, a family of sets of linear equations for the  $a$ 's, the T-matrix theories.

Equations (6) and (7) specify the boundary conditions at the surface of a scatterer which is a homogeneous inclusion. For the moment we will further simplify the problem by restricting the inclusion to be one of two kinds, either a void (cavity), for which the Dirichlet boundary condition of vanishing pressure

$$\phi(\vec{r}_+) = 0 \quad \text{void} \quad (12)$$

is satisfied, or a rigid fixed obstacle, for which the Neumann boundary condition of vanishing normal velocity

$$\hat{n} \cdot \vec{\nabla} \phi(\vec{r}_+) = 0 \quad \text{obstacle} \quad (13)$$

holds. The more general case is discussed in Section VI.

If Eq. (8) is substituted into Eqs. (12) and (13), the result is, where the arguments of the wavefunctions  $\phi$  are understood to be  $\vec{r}_+$ ,

$$\sum_s (d_s \tilde{\phi}_s + a_s \phi_s^{(+)}) = 0 \quad \text{void} \quad (14)$$

$$\sum_s (d_s \hat{n} \cdot \vec{\nabla} \tilde{\phi}_s + a_s \hat{n} \cdot \vec{\nabla} \phi_s^{(+)}) = 0 \quad \text{obstacle.} \quad (15)$$

Now we introduce a set of functions  $\{f_j\}$ ,  $j = 1, 2, \dots, \infty$  which is complete on  $\Sigma$ . Then if the notation

$$\int_\Sigma d\sigma \mathbf{u} \cdot \mathbf{v} = (\mathbf{u}, \mathbf{v}) \quad (16)$$

is introduced, Eqs. (14) and (15) when multiplied by  $f_j^*(\vec{r}_+)$  and integrated over  $\Sigma$  become

$$\sum_s \left[ (f_j, \tilde{\phi}_s) d_s + (f_j, \phi_s^{(+)}) a_s \right] = 0 \quad \text{void} \quad (17)$$

$$\sum_s \left[ (f_j, \hat{n} \cdot \vec{\nabla} \tilde{\phi}_s) d_s + (f_j, \hat{n} \cdot \vec{\nabla} \phi_s^{(+)}) a_s \right] = 0 \quad \text{obstacle} \quad (18)$$

Equations (14), (15) hold for every  $\vec{r}_+$  on the surface  $\Sigma$ ; because  $\{f_j\}$  is postulated to be complete on  $\Sigma$ , they are wholly equivalent to Eqs. (17), (18) for  $j = 1, 2, \dots, \infty$ .

These equations can be written in compact form

$$\tilde{Q}d + Qa = 0 \quad (19)$$

where

$$\tilde{Q}_{js} = \begin{cases} (f_j, \tilde{\phi}_s) & \text{void} \\ (f_j, \hat{n} \cdot \vec{\nabla} \tilde{\phi}_s) & \text{obstacle} \end{cases} \quad (20)$$

$$(21)$$

and

$$Q_{js} = \begin{cases} (f_j, \phi_s^{(+)}) & \text{void} \\ (f_j, \hat{n} \cdot \vec{\nabla} \phi_s^{(+)}) & \text{obstacle} \end{cases} \quad (22)$$

$$(23)$$

One can formally solve Eq. (19) for the vector a,

$$a = -Q^{-1}\tilde{Q}d = Td. \quad (24)$$

This defines the T-matrix which linearly transforms the incident wave amplitudes  $d_s$  into the outgoing wave amplitudes  $a_s$ .

The set of functions  $\{f_j\}$  with which one works in a practical calculation is, however, never complete. One has a basis set  $\{f_j\}$ ,  $j = 1, 2, \dots, L$ , where  $L$ , the truncation limit, is almost always significantly less than infinity. So although if  $L \rightarrow \infty$  the matrix equations are completely equivalent to the boundary conditions and  $T$  will not depend on what complete set  $\{f_j\}$  we choose, in practice  $L$  is rather small and the set must be chosen carefully. The sets  $\{\phi_s\}$  will also be truncated at  $s = L$ . This insures that the matrices  $Q$  are square, and we assume that  $Q^{-1}$  exists.

Conversely, our choice of the truncated set  $\{f_j\}_L$  will affect our calculated results, and we need to find some criterion to tell us which sets are better than others, and ideally to pick out an optimum one.

### III. MINIMUM PRINCIPLE

We would like to choose  $\{f_j\}_L$  so that the error in the results for physical observables is minimized. Because we do not know the exact values for cross-sections, we cannot formulate this condition. What we do know exactly are the boundary conditions, namely Eqs. (12) and (13), which the wavefunction  $\phi$  must satisfy. This leads us to consider the absolute squares of the deviance from the boundary conditions, integrated over the surface of the scatterer.

$$I = \begin{cases} (\phi, \phi) & \text{void} \\ (\hat{n} \cdot \vec{\nabla} \phi, \hat{n} \cdot \vec{\nabla} \phi) & \text{obstacle} \end{cases} \quad (25)$$

$$(26)$$

### Method of Optimal Truncation

I vanishes if and only if  $\phi$  satisfies the boundary conditions exactly, which happens in fact only if  $L \rightarrow \infty$ . For finite  $L$ ,  $I > 0$ , and we require that  $I$  be minimized with respect to variations in the coefficients  $a_s$ . We substitute Eq. (8) into Eqs. (25) and (26). If the resultant bilinear expression in the  $a$ 's has a minimum, then the derivatives

$$\frac{\partial I}{\partial a_s^*} = 0 \quad s = 1, 2, \dots, L, \quad (27)$$

must vanish. Computing them we find

$$\frac{\partial I}{\partial a_s^*} = \frac{\partial}{\partial a_s^*} \int_{\Sigma_1} d\sigma \left\{ \begin{array}{ll} |\phi_{\text{inc}} + \sum_{s'=1}^L a_{s'} \phi_{s'}^{(+)}|^2 & \text{void} \quad (28) \\ |\hat{n} \cdot \vec{\nabla} \phi_{\text{inc}} + \sum_{s'=1}^L a_{s'} \hat{n} \cdot \vec{\nabla} \phi_{s'}^{(+)}|^2 & \text{obstacle} \quad (29) \end{array} \right.$$

which are Eqs. (17), (18) with

$$f_s = \left\{ \begin{array}{ll} \phi_s^{(+)} & \text{void} \quad (30) \\ \hat{n} \cdot \vec{\nabla} \phi_s^{(+)} & \text{obstacle} \quad (31) \end{array} \right.$$

Equation (30), (31) specify one choice out of an infinite number which could be made for  $\{f_s\}$ . Waterman (1,2) using a very different approach, would prescribe

$$f_s = \left\{ \begin{array}{ll} \hat{n} \cdot \vec{\nabla} \tilde{\phi}_s & \text{void} \quad (32) \\ \tilde{\phi}_s & \text{obstacle} \quad (33) \end{array} \right.$$

for this scalar example. One needs to ask now: which of Eqs. (30), (31) or (32), (33), or of an infinite variety of others, will give the most accurate and reliable answers with least labor? This question can really only be satisfactorily answered by trying them and comparing the numbers obtained with different choices of  $\{f_s\}_L$ .

We will do this for a few choices in Section V, but one fact, a priori, does favor Eqs. (30), (31). Namely, this choice, because it results from a minimum principle, yields a convergent sequence of approximations, as we now prove.

#### IV. CONVERGENCE AND OTHER CRITERIA OF CHOICE

Consider the surface integral Eqs. (25), (26)

$$I_L = I(a_1, a_2, \dots, a_L, 0, 0, \dots) \quad (34)$$

to be a function of an infinite number of amplitudes  $a_s$ , with constraints

$$a_{L+1} = a_{L+2} = \dots = 0 \quad (35)$$

William M. Visscher

For  $L < \infty$ ,  $I_L > 0$ , and we know that if an exact solution exists, then the minimum value of  $I$  is zero for  $L \rightarrow \infty$ . Now define  $I_L^{\min}$  to be the minimum value of  $I_L$  which is attained by variation of its  $L$  complex arguments  $a_s$ , that is

$$I_L^{\min} = \min [I(a_1, a_2, \dots, a_L, 0, 0 \dots)] \quad (36)$$

Call the values of  $a_1 \dots a_L$  for which the minimum is attained  $a_1^{(L)}$ ,  $a_2^{(L)}$ ,  $\dots$ ,  $a_L^{(L)}$ ; i.e.

$$I_L^{\min} = I(a_1^{(L)}, a_2^{(L)}, \dots, a_L^{(L)}, 0, 0 \dots). \quad (37)$$

Now consider

$$I_{L+1}^{\min} = \min [I(a_1, a_2 \dots a_L, a_{L+1}, 0, \dots)] \quad (38)$$

then, because  $(a_1^{(L)}, a_2^{(L)}, \dots, a_L^{(L)}, 0)$  is a possible set of values of  $(a_1, a_2, \dots, a_{L+1})$  in Eq. (38), it follows that

$$I_{L+1}^{\min} \leq I_L^{\min}, \quad (39)$$

and  $I_L^{\min}$  forms a sequence which converges monotonically to zero as  $L \rightarrow \infty$ .

From the fact that a particular sequence of bilinear forms in the  $a_s$ 's converges monotonically to the exact answer, it does not necessarily follow that other bilinear forms, such as the cross-sections, are also convergent. But it is reasonable that they are. The coefficients of the bilinear form  $I_L$  are  $Q$ -matrix elements, whose magnitudes become very large when partial waves with high radial eigenvalue  $\ell$  are involved. On the other hand, the coefficients in the bilinear form for the cross-section  $\sigma$  do not increase rapidly with  $\ell$ . Therefore  $I_L$  is more sensitive than  $\sigma$  to changes in  $a_s$  for large  $s$ , and the latter should converge faster as  $L \rightarrow \infty$ . That it does so will be illustrated for a particular case in Section V.

The minimization of  $I$  [Eqs. (25)(26)] leads uniquely to a set  $\{f_s\}$  given by Eqs. (30), (31), which in turn leads to a monotonically convergent sequence  $I_L, I_{L+1}, \dots$ . But one could use other criteria for choosing  $\{f_s\}$ . Examples are energy conservation and satisfaction of reciprocity (7,2).

In any non-dissipative system energy is conserved. In a scattering process this implies the optical theorem, which is a proportionality between the imaginary part of the forward scattering amplitude and the total cross-section. In different terms it implies unitarity of the  $S$ -matrix (8).

The optical theorem imposes a constraint on the truncated amplitudes, which will thereby be overdetermined, because they are already uniquely specified by the matrix equation [Eq. (24)]. Alternatively, one can try to choose  $\{f_s\}$  so as to yield a unitary truncated  $S$ -matrix. This can be done (8), but not consistently with the minimization of  $I$ , which already uniquely determines  $\{f_s\}$ .

One manifestation of reciprocity is, in the scattering problem, that if the directions of observation and of the incoming wave are reversed and interchanged (i.e.  $\theta \leftrightarrow \pi - \theta_0$ ,  $\phi \leftrightarrow \pi + \phi_0$ ), then the cross-section is unchanged. Reciprocity is true

## MOOT

more generally than unitarity; the system need not, for example, be conservative. Reciprocity is guaranteed if the T-matrix (or the S-matrix) is symmetric.

Reciprocity imposes another condition on the truncated amplitudes; again it cannot be satisfied simultaneously with minimization of I.

One might choose to satisfy the minimization principle exactly and use the other symmetries to check the accuracy of the results. Or one might choose to satisfy the symmetries exactly and the matrix equations approximately. A third alternative is to solve the overdetermined system in a least-squares sense, satisfying everything only approximately.

We take the first course. Waterman (2) effectively took the second. Possibly the third course would be advantageous, but it is more complicated and as yet untried.

### V. NUMERICAL EXAMPLES AND COMPARISONS

The T-matrix [Eq. (24)] is given by  $T = -Q^{-1}\tilde{Q}$ , where

$$\begin{aligned} Q_{ss'} &= \left( \phi_s^{(+)} , \phi_{s'}^{(+)} \right) \\ \tilde{Q}_{ss'} &= \left( \phi_s^{(+)} , \tilde{\phi}_{s'} \right) \end{aligned} \quad (40)$$

and  $s = (\ell, m)$ ;  $\ell = 0, 1, \dots, \ell_{\max}$ ;  $m = -\ell, -\ell+1, \dots, \ell$ . For nonspherical shapes these matrix elements must be calculated numerically, which comprises most of the computational labor in a scattering calculation. An important simplification is obtained if the shape  $\Sigma$  is constrained to be axially symmetric. Then it is clear from Eq. (10) that the Q and  $\tilde{Q}$  matrices are diagonal in m;

$$Q_{\ell m, \ell' m'} = \delta_{mm'} Q_{\ell m, \ell' m} = \delta_{mm'} Q_{\ell -m, \ell' -m} \quad (41)$$

where the second equality follows from

$$Y_{\ell -m} = (-1)^m Y_{\ell m}^* \quad (42)$$

Thus the Q-matrices can be rearranged as follows,

$$Q = \begin{pmatrix} Q^{(0)} & 0 & & 0 \\ 0 & Q^{(1)} & & \\ 0 & & \ddots & 0 \\ 0 & & & Q^{(\ell_{\max})} \end{pmatrix} \quad (43)$$

which represents a block-diagonal matrix, wherein matrices along the diagonal are

William M. Visscher

$$Q^{(m)} = \begin{pmatrix} Q_{mm,mm} & Q_{mm,m+1} & \dots & Q_{mm,\ell_{\max}^m} \\ \cdot & \cdot & \cdot & \cdot \\ \cdot & \cdot & \cdot & \cdot \\ Q_{\ell_{\max}^m,mm} & \dots & \dots & Q_{\ell_{\max}^m,\ell_{\max}^m} \end{pmatrix} \quad (44)$$

with  $Q^{(0)}$  being  $(\ell_{\max} + 1) \times (\ell_{\max} + 1)$  and  $Q^{(\ell_{\max})}$  being  $(1 \times 1)$ .

This is an important simplification because the inverses and products of block-diagonal matrices are again block-diagonal. Thus

$$Q^{-1} = \begin{pmatrix} Q^{(0)-1} & 0 & 0 & 0 \\ 0 & \cdot & \cdot & 0 \\ 0 & \cdot & \cdot & 0 \\ 0 & 0 & 0 & Q^{(\ell_{\max})^{-1}} \end{pmatrix} \quad (45)$$

and

$$T = \begin{pmatrix} T^{(0)} & 0 & 0 & 0 \\ 0 & \cdot & \cdot & 0 \\ 0 & \cdot & \cdot & 0 \\ 0 & 0 & 0 & T^{(\ell_{\max})} \end{pmatrix} \quad (46)$$

where

$$T^{(m)} = -Q^{(m)-1} \tilde{Q}^{(m)} \quad (47)$$

Therefore the T-matrix, and hence the amplitudes  $a_{\ell m}$ , can be calculated separately for each  $m$ . The largest matrix we ever need to invert or multiply has rank  $(\ell_{\max} + 1)$ , which is the square root of the rank of the T-matrix for a shape with no symmetries.

It should be emphasized that although we have taken the axis of symmetry of the scatterer to be in the z-direction neither the incoming plane wave nor the direction of observation are constrained. The T-matrix does not depend on  $\theta_0, \phi_0$ ; once we have calculated T we can immediately get the scattered amplitudes for any incident direction, viz, from Eq. (9),

$$\begin{aligned} a_{\ell m} &= \sum_{\ell'=m}^{\ell_{\max}} T_{\ell m, \ell' m}^{(m)} d_{\ell' m} \\ &= 4\pi \sum_{\ell'=m}^{\ell_{\max}} T_{\ell m, \ell' m}^{(m)} i^{\ell'} Y_{\ell' m}^*(\theta_0, \phi_0) \end{aligned} \quad (48)$$

### Method of Optimal Truncation

The differential cross-section  $\frac{d\sigma}{d\Omega}$  is the scattered power per unit solid angle divided by the incident power per unit area: it is easy to show that it is

$$\frac{d\sigma}{d\Omega} = k^{-2} \left| \sum_{\ell m} i^{-\ell-1} a_{\ell m} Y_{\ell m}(\theta, \phi) \right|^2 \quad (49)$$

Although the equations we have written have been exclusively for the scalar case, similar ones, with more components, can be written for elastic waves (4). The numerical results that we now present are for the latter case, which is more complicated because the elastic displacement is a vector. Thus the scalars in the surface integrals Eqs. (20)-(23) are replaced by the vectors

$$\rho \phi_{\ell m} \rightarrow \vec{S}_{p\ell m} \quad (50)$$

$$\hat{n} \cdot \vec{\nabla} \phi_{\ell m} \rightarrow \vec{t}_{p\ell m}, \quad (51)$$

and scalar products are taken in the integrals.  $\vec{S}$  and  $\vec{t}$  are the displacement and surface traction (stress tensor contracted with  $\hat{n}$ ) vectors respectively. The radial and azimuthal eigenvalues have been supplemented by a polarization  $p = 1$  (longitudinal), 2,3 (transverse).

#### Comparison Between Different Basis Sets $\{f_s\}_L$ .

The case we consider here is the scattering of a longitudinally polarized elastic wave incident at  $45^\circ$  on an oblate spheroidal void. The prescription of MOOT for this case is

$$f_s = \vec{t}_{p\ell m}^{(+)} \quad (52)$$

where, again, the (+) means that the surface traction is constructed from outgoing waves. But several other choices besides Eq. (52) suggest themselves as being just as easy to calculate with, to wit,

$$f_s = \begin{cases} \vec{S}_{p\ell m} & (53a) \\ \vec{t}_{p\ell m} & (53b) \\ S_{p\ell m}^{(o)} & (53c) \\ t_{p\ell m}^{(o)} & (53d) \\ S_{p\ell m}^{(t)} & (53e) \\ t_{p\ell m}^{(+)} & (53f) \end{cases}$$

William M. Visscher

The first two are constructed from regular Bessel functions, the last two from outgoing waves (Hankel functions) and the middle two have no  $r$  dependence, but are merely linear combinations of vector spherical harmonics, obtained by setting  $r = a$  in Eqs. (53a) and (53b).

Figure 2 shows computed results for the total longitudinal cross-section for all of these choices for  $ka = 1$  ( $a$  is the radius of the oblate spheroid, which in this figure has aspect ratio 2/3). These results support the view that for this scattering situation, at least, the outgoing waves (e) and (f) are to be preferred. This choice is reinforced by the results shown in Fig. 3, which is the same as the preceding one except that the oblate spheroidal void now has aspect ratio 1/2. Whether or not the surface traction (f) is superior to the displacement (e) is not decided by this data. On subjective esthetic grounds we prefer (f); it is prescribed by MOOT.

#### Convergence of Truncation Sequence

As discussed above, the sequence of surface integrals  $I_L, I_{L+1}, \dots$  converges monotonically. It is of interest to see for a particular case just how fast the convergence is, and how it is correlated with the convergence of an observable cross-section. Numerical results are presented in Fig. 4 for scattering of an incident longitudinal wave from a sphere and from a prolate spheroidal fixed rigid obstacle. They confirm the monotonic convergence of  $I$ , and indicate that the sequence of approximations to the cross-section converge much faster, albeit not monotonically.

#### Examples of Differential Cross-Sections

Scattering of an incident longitudinal wave with  $ka = 10$  from a conical void in titanium is shown in Fig. 5. This cone has radius equal to its height; the incident direction is  $(\theta_0, \phi_0) = (135^\circ, 0^\circ)$ . Peaks appear in the longitudinal cross-section both in the forward and the specularly reflected directions.

Mode-converted scattering of an incident longitudinal wave from an oblate spheroidal void in titanium is shown in Fig. 6. Again  $ka = 10$ , but  $(\theta_0, \phi_0) = (90^\circ, 0)$ . The incident wave is longitudinally polarized here; the boundary produces a transversely polarized component in the scattered wave (mode conversion). Symmetry requires that the cross-section vanish in the forward and backward directions; these points are plotted at -100 db.

Figure 7 has geometry similar to that of Fig. 6, but the target is now a pillbox with aspect ratio 1/2 (height = radius). The forward peak has diffraction minima surrounding it, and there is evidence of specular reflection from the pillbox side. The longitudinal cross-section is the ordinate.

Spot checks on the consistency of our results with the optical and reciprocity theorems have been made. Both agree within about 1/2 db for oblate spheroidal voids with aspect ratio 1/2 and  $ka \leq 2$ . Agreement deteriorates for larger  $ka$  and more extreme shapes because the angular variation becomes more rapid.

## VI. INCLUSIONS AND CRACKS

Referring again to Fig. 1, we imagine that  $\Sigma$  is filled with a compressible irrotational fluid with density  $\rho'$  and compressibility  $\kappa'$ , and the conditions that

MOOT

must be satisfied at the boundary are given by Eqs. (6) and (7). In analogy with Eqs. (25), (26) we form the surface integrals

$$I = \int_{\Sigma} |\rho' \phi(\vec{r}_-) - \rho \phi(\vec{r}_+)|^2 d\sigma \quad (54)$$

$$J = \int_{\Sigma} |\hat{n} \cdot \vec{\nabla} \phi(\vec{r}_-) - \hat{n} \cdot \vec{\nabla} \phi(\vec{r}_+)|^2 d\sigma, \quad (55)$$

and we need an additional expansion for the wave function inside the defect. So for  $\vec{r}$  inside  $\Sigma$  we put

$$\phi(\vec{r}) = \sum_s a'_s \tilde{\psi}_s(\vec{r}), \quad (56)$$

where only the regular solutions of the inside Helmholtz equation

$$(\nabla^2 + k'^2) \psi_s(\vec{r}) = 0 \quad (57)$$

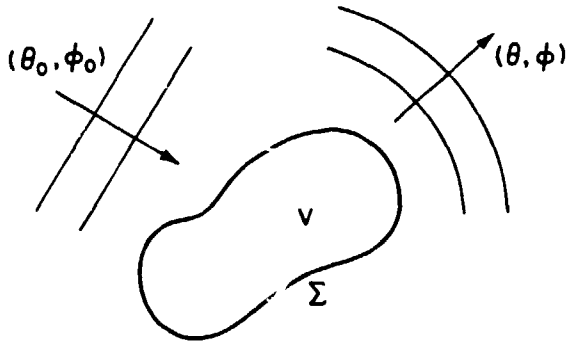


Fig. 1. Scattering geometry. A homogeneous flaw of volume  $V$  with a surface  $\Sigma$  is imbedded in the host medium. A wave is incident with wavenumber  $k$  at polar and azimuthal angles  $(\theta_0, \phi_0)$ . Spherical outgoing scattered waves emanate from the flaw: the direction of observation is  $(\theta, \phi)$ .

contribute, because the origin is always assumed to be inside  $\Sigma$ . Now both  $I$  and  $J$  are bilinear forms in  $a_s$  and  $a'_s$ , a total of  $2L$  amplitudes. We can solve for them as follows. Form a positive definite linear combination of  $I$  and  $J$ :

$$K = \alpha I + (1 - \alpha)J, \quad (58)$$

with  $0 \leq \alpha \leq 1$  and minimize  $K$  with respect to variations in  $a_s$  and  $a'_s$ .

$$\frac{\partial K}{\partial a_s} = 0 \quad (59)$$

$$\frac{\partial K}{\partial a'_s} = 0 \quad (60)$$

Equations (59) and (60) are both matrix equations for the amplitude vectors  $\vec{a}$  and  $\vec{a}'$  in  $L$  dimensions; the matrices occurring in them are surface integrals like  $Q$  and  $\tilde{Q}$  (Eqs. (20)-(23)).

With the definitions

William M. Visscher

$$\begin{aligned}
 Q &= \begin{pmatrix} \rho\phi^{(+)} & \rho\phi^{(+)} \\ \rho\phi^{(+)} & \rho\tilde{\phi} \end{pmatrix} \\
 \tilde{Q} &= \begin{pmatrix} \rho\phi^{(+)} & \rho\tilde{\phi} \\ \rho\phi^{(+)} & \rho'\tilde{\psi} \end{pmatrix} \\
 Q' &= \begin{pmatrix} \rho\phi^{(+)} & \rho'\tilde{\psi} \\ \rho'\tilde{\psi} & \rho'\tilde{\psi} \end{pmatrix} \\
 Q'' &= \begin{pmatrix} \rho'\tilde{\psi} & \rho'\tilde{\psi} \\ \rho'\tilde{\psi} & \rho\tilde{\phi} \end{pmatrix} \\
 \tilde{Q}' &= \begin{pmatrix} \rho'\tilde{\psi} & \rho\tilde{\phi} \end{pmatrix},
 \end{aligned} \tag{61}$$

and a set  $R, \tilde{R}, \dots$ , which is the same as  $Q, \tilde{Q}, \dots$  except  $\rho$  (and  $\rho'$ ) is replaced with  $\hat{n} \cdot \hat{v}$ , we construct a set of matrices  $P, \tilde{P}, \dots$  according to

$$P = \alpha Q + (1 - \alpha)R. \tag{62}$$

Then Eqs. (59) and (60) can be written

$$P'\vec{a}' - \tilde{P}\vec{d} - P\vec{a} = 0 \tag{63}$$

$$P''\vec{a}' - \tilde{P}'\vec{d} - P'\vec{a} = 0, \tag{64}$$

and the unobserved interior amplitudes  $\vec{a}'$  eliminated;

$$\begin{aligned}
 \vec{a} &= -\left[P - P'P''^{-1}P'\right]^{-1} \left[\tilde{P} - P'P''^{-1}\tilde{P}'\right] \vec{d}. \\
 &= T \vec{d}
 \end{aligned} \tag{65}$$

This equation still contains the parameter  $\alpha$ , which can be chosen to affect one or more of a number of things: 1) the matrices which must be inverted may be ill-conditioned for some values of  $\alpha$ , 2) the rate of convergence of the truncation sequence will depend on  $\alpha$ , 3) the accuracy as reflected by how well the optical theorem and/or reciprocity are satisfied will depend on  $\alpha$ .

Cracklike defects present a special problem in a scattering calculation. One might hope that a crack could be considered to be the limit of a void as opposite sides squeeze together and the volume goes to zero. This introduces serious problems in the partial wave expansion, because the origin must be inside the crack, and the outgoing partial waves contain irregular Bessel functions. So we would like to consider the crack to be part of a surface which has a mathematical interior. Thus consider Fig. (8), which depicts our view of a plane circular crack. It is simulated by a truncated spherical inclusion, for which the included material is identical to that outside, and the boundary conditions imposed are free-surface both inside and outside on the plane circle, and continuity of both displacement and surface traction is required over the spherical surface.

A straightforward treatment of the crack as a special case of the inclusion is foiled by a well-known feature of displacements and stresses in the neighborhood of a crack edge. Namely, they are singular, the displacements behaving like  $\epsilon^{-2}$ , the stresses like  $\epsilon^{-3}$ , where  $\epsilon$  is the distance from the field point to the edge of the crack. The futility of attempting to describe these with a partial-wave expansion is manifest; fortunately exact solutions in the neighborhood of the edge are known in terms of a small number of parameters. Using them, work on the application of MOOT to cracks is in progress and will be reported elsewhere.

#### Acknowledgements

Continued interactions with Dr. James E. Gubernatis have been generally informative and often useful.

### Method of Optimal Truncation

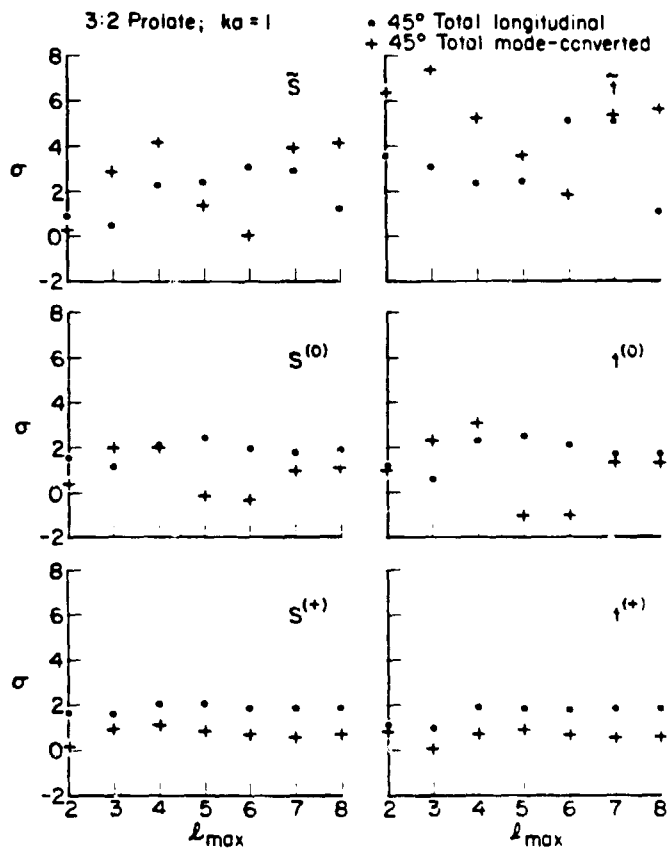


Fig. 2. Total longitudinal (•) and total mode-converted (+) cross-sections for scattering of an incident longitudinal wave with  $ka = 1$  at  $(\theta_0, \phi_0) = (45^\circ, 0^\circ)$  from an ~~oblate~~ prolate spheroidal void with aspect ratio 2/3. Six different choices are made for  $f_s$  as discussed in the text, the abscissa is the truncation limit  $l_{max}$ , and the cross-sections, divided by  $\pi a^2$ , are plotted in db.

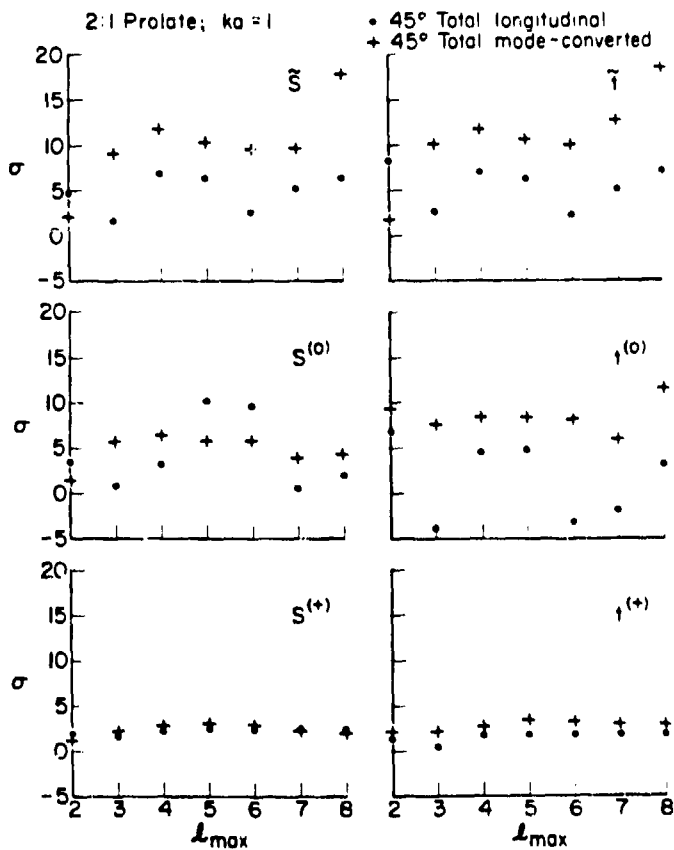


Fig. 3. Same as Fig. 2, but the void now has aspect ratio 1/2. The accuracy of most of the results here has deteriorated; note the change of scale in the ordinate.

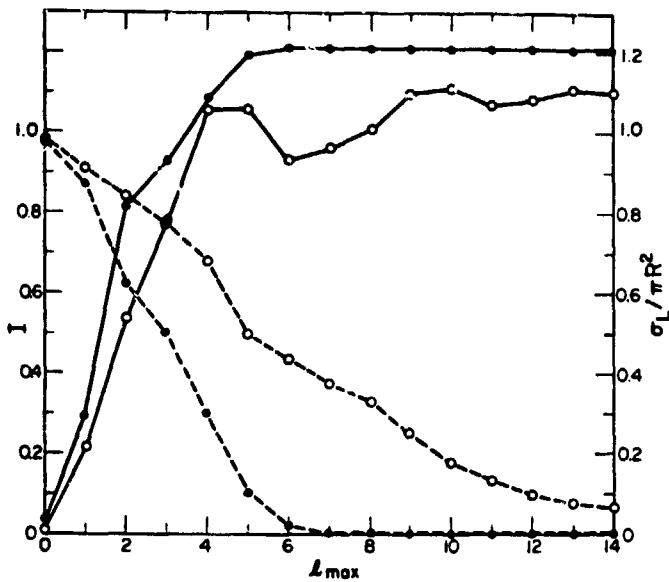


Fig. 4. Normalized surface integrals  $I$  (dashed lines) of the square of the vector displacement for scattering from spherical ( $\bullet$ ) and prolate spheroidal ( $\circ$ ) rigid obstacles. Also shown are calculated total longitudinal cross-sections for  $(\theta_0, \phi_0) = (45^\circ, 0^\circ)$ . The incident wave is longitudinal with  $ka = 5$  ( $a =$  radius of the sphere); the spheroid has aspect ratio 2/1 and has the same volume as the sphere.

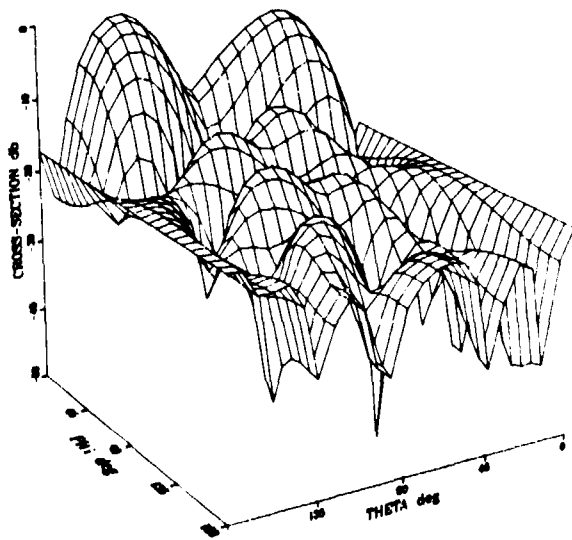


Fig. 5. Differential longitudinal cross-section for a right circular conical void with aspect ratio 1/2. The cone has its flat side up and  $(\theta_0, \phi_0) = (135^\circ, 0^\circ)$ ; thus a specular reflection would be expected at  $(\theta, \phi) = (45^\circ, 0^\circ)$ . The medium is titanium; the incident wave is longitudinally polarized and has  $ka = 10$ .

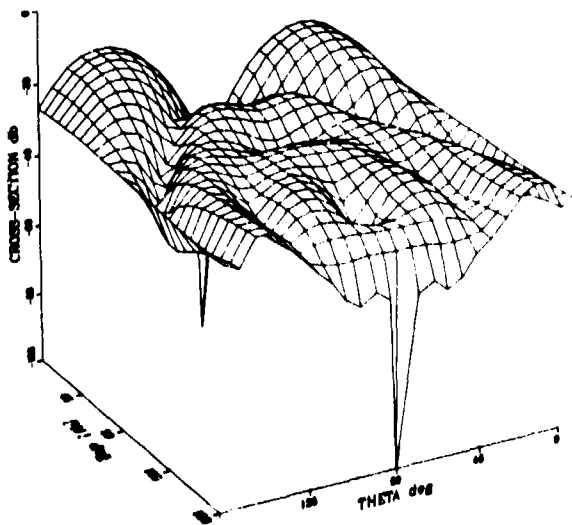


Fig. 6. Differential mode-converted cross-section for scattering of a longitudinal wave incident at  $(\theta_0, \phi_0) = (90^\circ, 0^\circ)$  with  $ka = 10$  from an oblate spheroidal void (aspect ratio 1/7) in titanium. Symmetry requires the cross-section to vanish in the forward and backward directions; it is plotted at -100 db.

MOOT

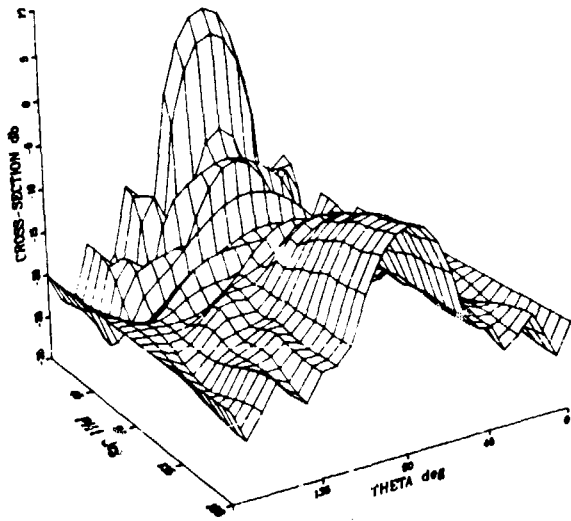


Fig. 7. Longitudinal scattering from a pillbox-shaped void in titanium. The incident wave has  $ka = 10$  and  $(\theta_0, \phi_0) = (90^\circ, 0^\circ)$ ; the aspect ratio is  $1/2$ .

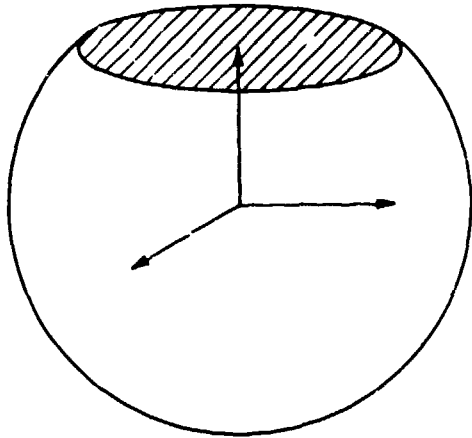


Fig. 8. Simulation of a circular crack by an identical inclusion. Continuous boundary conditions are imposed everywhere except on the cross-hatched circle where free-surface boundary conditions are imposed both from above and from below.

REFERENCES

1. P. C. Waterman, J. Acoust. Soc. Am., 45, 1418 (1968).
2. P. C. Waterman, J. Acoust. Soc. Am., 60, 567 (1976).
3. V. Varatharajulu and Y.-H. Pao, J. Acoust. Soc. Am., 60, 556 (1976).
4. See William M. Visscher, J. Appl. Phys. (in press) or Los Alamos Preprint LA-UR-79-399 for details of the formulation for elastic waves.
5. E. U. Condon and H. Odishaw, eds., "Handbook of Physics" (McGraw-Hill, N.Y. 1967), Part 3, Chapter 7 by P. M. Morse.
6. J. D. Jackson, "Classical Electrodynamics" (Wiley, N.Y., 1962), Chapter 3.
7. V. Varatharajulu, J. Math. Phys. 18, 537 (1977).
8. William M. Visscher, loc. cit. and Los Alamos Preprint LA-UR-78-3008.